Comparative Dual-Tracer Studies of Carbon-14 Tryptophan and Iodine-131 HIPDM in Animal Models of Pancreatic Diseases

Kazuo Kubota, Prantika Som, A. Bertrand Brill, Donald F. Sacker, George E. Meinken, Suresh C. Srivastava, and Harold L. Atkins

Brookhaven National Laboratory, Upton, New York; and State University of New York at Stony Brook, Stony Brook, New York

Our previous studies have shown that a significant amount of the diamine derivative ^{131}I-N,N,N′-trimethyl-N′-(2-hydroxy-3-methyl-5-iodobenzyl)-1,3-propanediamine (HIPDM) is taken up and retained by the normal pancreas. Therefore, we studied the uptake of [^{131}I]HIPDM in various pathophysiological models in mice (chronic alcoholism, diabetes with beta-cell atrophy and obesity with beta-cell hypertrophy) and compared to ^{14}C-L-Tryptophan (TRY) distribution in order to determine the factors influencing their pancreatic uptake. In normal animals, the pancreas uptake of TRY was generally higher than HIPDM. In diabetes, the relative concentration of both compounds was higher over the controls; however, in obesity, TRY showed lower accumulation than in controls while HIPDM showed no significant difference. Chronic ethanol (20%) ingestion increased TRY uptake in the pancreas compared to controls (36.88 ± 3.21 vs. 30.03 ± 4.17% ID/g; $p < 0.01$) after 5 wk study period, but it decreased by 10 wk (22.36 ± 0.95% ID/g; $p < 0.005$). There were no significant changes in [^{131}I]HIPDM distribution in alcoholics as compared to the controls. Radioiodinated HIPDM has potential advantages over [^{11}C]TRY for pancreatic imaging since conventional imaging techniques can be employed. Our data, however, suggest that ^{11}C-L-TRY is a more sensitive indicator of various pancreatic disorders.

J Nucl Med 30:1848–1855, 1989

Pancreatic imaging by computerized tomography (CT) and endoscopic retrograde cholangiopancreatography (ERCP) contributed to improved diagnosis of pancreas diseases. However, ERCP is an invasive and time-consuming technique, and accurate diagnosis in the early stage of disease remains difficult.

After extensive clinical investigations, selenium-75 (^{75}Se) selenomethionine was discarded as a pancreas scanning agent (*1*) by many centers by the end of the 1970s (*2*) mainly because the poor physical properties of ^{75}Se (high gamma-ray energy, long half-life, high radiation absorbed dose). In search for better agents, several carbon-11-(^{11}C) labeled amino acids and their derivatives have been tested for the delineation of pancreas in animals and humans, and the most promising of these tracers was found to be [^{11}C]tryptophan (TRY) (*3–5*). However, clinical use of [^{11}C]TRY is limited because of extensive facilities and resources needed for positron tomography (imaging devices, in-house cyclotron and extensive support for radiopharmaceutical production).

Recently, high pancreas affinity of iodine-131-(^{131}I) labeled N,N,N′-trimethyl-N′-(2-hydroxy-3-methyl-5-iodobenzyl)-1,3-propanediamine (HIPDM) similar to amino acids have been observed in normal mice and rats, and it was suggested that HIPDM could be a potentially useful pancreas imaging agent using conventional scintigraphy (*6*). However, the mechanisms of pancreas uptake and the effects of pancreas pathology on the radioiodinated HIPDM uptake remain to be elucidated. We therefore performed a comparative study of [^{131}I]HIPDM with ^{14}C-L-TRY (as a substitute for ^{11}C) in various pancreas pathology models (chronic alcoholic mice, diabetic mice, obese mice), and cancer to answer the following questions: Is HIPDM pancreas uptake altered in different disease models? Which is the better agent for pancreas imaging?

Received July 11, 1986; revision accepted July 21, 1989.

For reprints contact: P. Som, MD, Medical Dept., Brookhaven National Laboratory, Upton, NY 11973.

MATERIALS AND METHODS

Radioisotope

Radioiodination of HIPDM using ^{131}I as a substitute for ^{123}I was carried out as described previously (*6*). L-[carboxyl-^{14}C]-tryptophan (specific activity 55 mCi/mmol, radiochemical purity 98.1% to 97.1%, optical purity 98.1%) was purchased from Amersham Corporation (Arlington Heights, IL) and used as a substitute for L-[carboxy-^{11}C]-tryptophan (*7*).

Animals

Chronic alcoholic mice. Hale Stoner strain Swiss BNL adult female mice (5-wk-old) were divided into two groups. One group of 41 mice had free access to water and served as the controls. The other group of 41 mice were given 20% (V/V) ethanol as the sole drinking fluid. Both groups were given standard laboratory food ad libitum. During the fifth and tenth week after ethanol treatment, isotope experiments were carried out.

Diabetic and obese mice. Eight-week-old female C57BL/KsJ-db/db (*8*) diabetic and control mice; and C57BL/6J-ob/ob (*9*) obese and control mice were obtained from Jackson Laboratory (Bar Harbor, ME) and used for experiments at 9 to 10 wk of age.

Tumor animals. Spontaneous mammary adenocarcinoma derived from Hale-Stoner strain Swiss BNL mice maintained by bi-weekly subcutaneous transplantation was used 2 wk following inoculation when the tumor size became 0.5-1 cm diameter.

Experiment

Tissue distribution. Iodine-131 HIPDM or [^{14}C]TRY (2-3 μCi in 0.2 ml saline) was injected intravenously through the tail vein. Time course tissue distribution of [^{14}C]TRY was performed to compare with the reported [^{131}I]HIPDM distribution (*6*) and also to determine the best time for comparative study. Based on these data, a 60-min killtime was chosen for subsequent experiments. After killing, the tissue samples were excised, blotted to remove blood, weighed and counted in a well-type NaI(T1) scintillation counter (Auto-Gamma Scintillation Spectrometer, Packard).

Double tracer autoradiography (ARG). One-hundred microliters of [^{131}I]HIPDM (0.1 ml), and 2.5 μCi of [^{14}C]TRY (0.2 ml) were mixed and injected into the mice through the tail vein. The mice were killed 1 hr after injection, processed for whole body autoradiography (*10,11*) and the whole body sections were exposed to x-ray film (Lo-Dose mammography film, DuPont). The first 6-hr exposure to film yielded images of shorter-lived ^{131}I. The tissue sections were then retained for three months to allow for decay of ^{131}I (greater than 10 half-lives) and then the sections were reexposed to film for two weeks to obtain images of the distrubtion of the longer-lived ^{14}C.

Protein incorporation. Incorporation of [^{14}C]TRY into the crude protein fraction was measured as follows: tissue samples were homogenized with 10% trichloroacetic acid (TCA), centrifuged for 5 min at 2500 rpm twice. Then the pellets were washed twice with ethanol-ether (3:1), washed once with acetone, dried overnight and weighed. The pellets were then digested with 0.4 ml of 30% hydrogenperoxide-70% perchloric acid (3:1) and incubated at 80°C for 2 hr. The supernatants were extracted by six times volume of ether and water fraction made up to a fixed volume (10 ml). Digested pellets and aliquots of supernatants were mixed with 12 ml of liquid scintillation cocktail (ACSII, Amersham), shaken vigorously, stored overnight at room temperature and then counted in a liquid scintillation counter (Beckman #LS7800f).

Blood chemistry. Blood samples of mice were obtained by decapitation for the measurements of serum cholesterol, glucose, amylase, and aspartate aminotransferase (AST). All measurements were done using an automatic analyzer (Technicon RA-1000 system, Technicon Instruments Corporation, New York).

RESULTS

Figure 1 shows the time course tissue distribution of [^{131}I]HIPDM and [^{14}C]TRY. Pancreas uptake of [^{14}C]TRY increased rapidly and reached peak at 60 min after injection at which time the liver/pancreas ratio was the highest. Percent TCA pellet activity was almost saturated at 60 min after injection and more than 90% of the pancreas radioactivity was incorporated into crude protein fraction. Blood radioactivity for both [^{14}C]TRY and [^{131}I]HIPDM cleared very rapidly. HIPDM uptake by the liver and pancreas was equal at 5 min, then the pancreas uptake rose gradually until 2

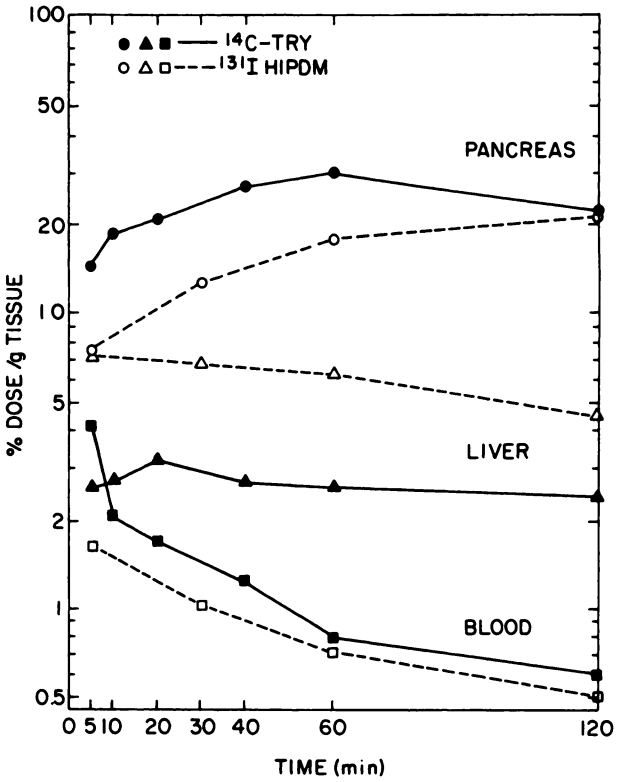

FIGURE 1
Time course tissue distribution of [^{14}C]TRY and [^{131}I] HIPDM in normal mice. Ordinate is percent injected dose per gram of tissue. Closed symbols with solid lines are [^{14}C]TRY, open symbol with broken lines are [^{131}I]HIPDM.

hr. Based on these data, a 60 min study time was selected for subsequent experiment. If TRY was labeled with ^{11}C for clinical application 60 min could be the maximum time limit because of its short half-life (20 min), moreover, the radioactivity of both tracers excreted in the intestine at later time period might interfere with pancreas image.

Figure 2 depicts the double tracer whole body autoradiography (WBARG) of the normal mice (C57BL) with [^{14}C]TRY and [^{131}I]HIPDM. The similarities and differences in the whole body distribution of [^{131}I] HIPDM and [^{14}C]TRY at 1 hr postinjection is clearly demonstrated by WBARG technique. WBARG with HIPDM showed very high brain uptake and the lung showed almost the same radioactivity as did the pancreas. Adrenal uptake was slightly higher than in the kidneys and high radioactivity was present in the intestinal contents at 1 hr after injection. Salivary gland, thymus, and liver also showed isotope accumulation. The highest accumulation of [^{14}C]TRY was seen in pancreas, and the intestines. Salivary gland, liver, and renal cortex also showed moderate isotope accumulation.

There was no significant differences in mean body weight between the alcoholic and their respective control groups. AST and amylase were significantly reduced after 10 wk of alcohol treatment (AST; control 164 ± 47 mU/ml, alcoholic 114 ± 25 mU/ml, amylase; control 1223 ± 177 U/l, alcoholic 1052 ± 106 U/l). The changes of the isotope uptake by the liver and pancreas during the course of the alcohol treatment are shown in Figure 3. The accumulation of [^{14}C]TRY in the pancreas increased after 5 wk of alcohol intake. However, chronic alcohol drinking depressed pancreas uptake at values lower than control at the end of 10 wk treatment. The accumulation of [^{131}I]HIPDM remained unchanged after 10 wk of alcohol intake. These data suggest the pancreas distribution of [^{14}C]TRY is more sensitive to the effect of alcohol intake than [^{131}I] HIPDM. Both [^{14}C]TRY and [^{131}I]HIPDM uptake by the liver indicated no significant differences after the alcohol treatment. Table 1 shows the isotope accumu-

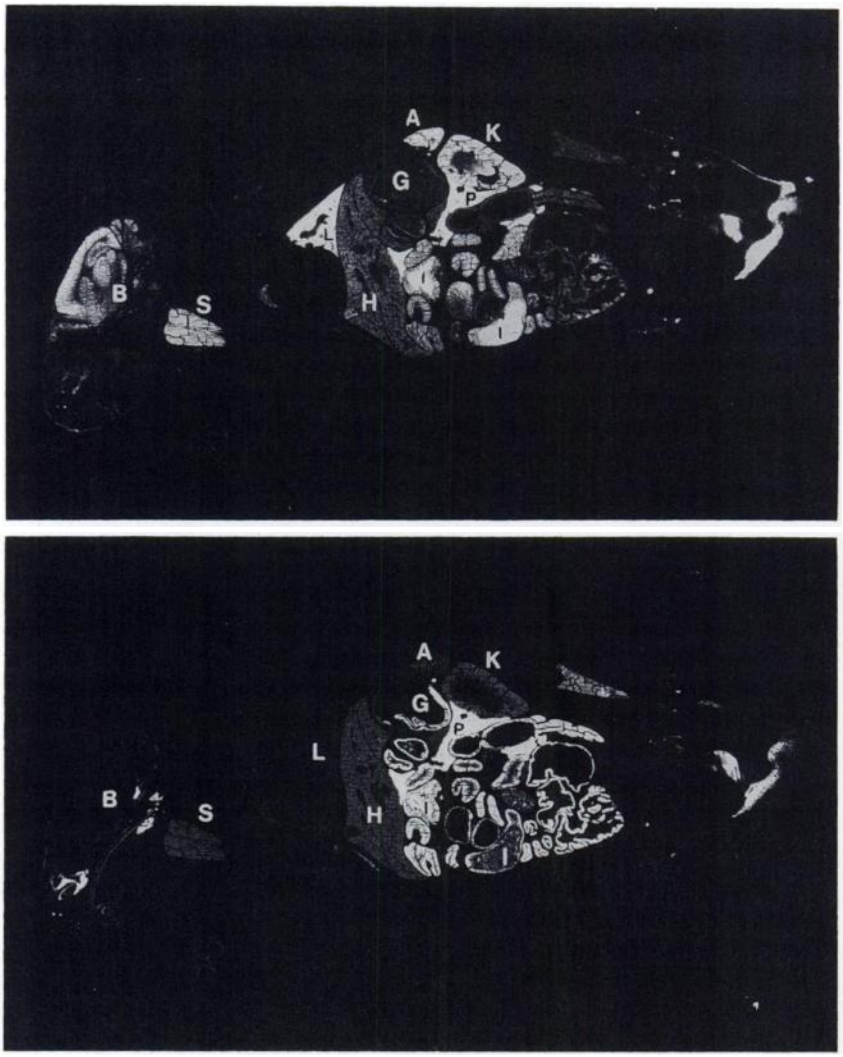

FIGURE 2
Double tracer whole-body autoradiography of the normal mice with [^{131}I] HIPDM and [^{14}C]TRY 60 min after i.v. injection. Both [^{131}I]HIPDM (upper) and [^{14}C]TRY (lower) images with the same symbols, brain, B; salivary gland, S; lung, L; liver, H; adrenal, A; kidneys, K; pancreas, P; intestine, I; stomach, G.

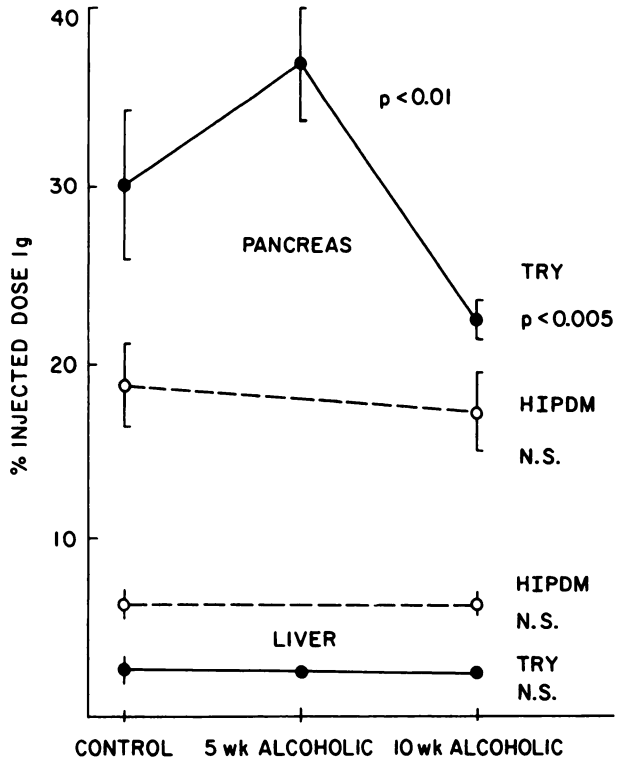

FIGURE 3
Effects of alcohol treatment on the isotopes uptake by the liver and pancreas. Ordinate is percent injected dose per gram of tissue. Closed symbols with solid lines are [^{14}C] TRY. Open symbols with broken lines are [^{131}I]HIPDM. All points on the curves are compared to the control and the results of Student's t-test are shown. N.S.: not significantly different.

lation for both tracers and % TCA pellet data for [^{14}C] TRY. Protein incorporation rate (% TCA pellet) of pancreas decreased after 10 wk, however, in the liver it decreased after 5 wk of alcohol treatment.

Table 2A, B shows the results of the experiments with the obese and diabetic mice. Glucose level was highest in the diabetic mice (control 234 ± 35 mg/dl, DM 712 ± 273, obesity 394 ± 104). Also, cholesterol level was higher in the diabetec and the obese mice (control 75 ± 11 mg/dl, DM 152 ± 25, obesity 136 ± 15). Since the body weight of the obese mice and the diabetic mice were twice that of respective control mice, relative concentration (previously described as differential uptake ratio) (*12*) which was normalized to body weight is used for comparison. In the obese mice, [^{14}C] TRY uptake by the pancreas (both % ID/g and relative concentration) was significantly decreased compared to the control, but the HIPDM relative concentration showed no significant differences. In the diabetic mice, pancreas relative concentration of [^{14}C]TRY and [^{131}I] HIPDM was higher than the controls. The liver relative concentration of [^{14}C]TRY and HIPDM increased in the diabetic mice but [^{14}C]TRY was decreased in the obese mice, while [^{131}I]HIPDM uptake remained unchanged.

Diabetic mice and obese mice are homozygote of two different mutant subline of C57BL mice, and each heterozygote of these subline served as the controls. Difference of these two control can be explained by the difference in the subline of mice.

Uptake of [^{14}C]TRY and [^{131}I]HIPDM in transplanted mammary adenocarcinoma is shown in Table 3. No significant difference was observed in the tumor uptake of [^{14}C]TRY and [^{131}I]HIPDM, neither agent showed significant tumor affinity and both were lower than that of liver and pancreas, but higher than blood and muscle. Tumor/tissue ratios of blood and muscle for [^{14}C]TRY were higher than with [^{131}I]HIPDM because of faster blood clearance and less muscle uptake by the former.

DISCUSSION

Functional imaging based on pathophysiologic changes of the organ rather than anatomical changes has been a unique characteristic of nuclear medicine science. A diagnostic screening scan similar to thyroid scanning has long been a goal in pancreas imaging.

TABLE 1
Effect of Alcohol Treatment on Tracer Accumulation and TCA Pellet Incorporation

	Pancreas uptake			Liver uptake		
	Tryptophan		HIPDM	Tryptophan		HIPDM
	% Dose/g	% TCA pellet‡	% Dose/g	% Dose/g	% TCA pellet	% Dose/g
Control (10)	30.03 ± 4.17*	97.5 ± 0.6	17.13 ± 2.17	2.58 ± 0.38	89.0 ± 2.8*	6.30 ± 0.58
5 wk Alcoholic (6)	36.88 ± 3.21*	97.8 ± 0.3*	—	2.55 ± 0.32	84.4 ± 2.4*	—
10 wk Alcoholic (6)	22.36 ± 0.95†	96.6 ± 0.7*	18.67 ± 2.39 (N.S.)	2.44 ± 0.22	83.9 ± 2.6*	6.34 ± 0.74 (N.S.)

N.S. = not significant.
* $p < 0.01$ (Student's t-test).
† $p < 0.005$.
‡ $\frac{\text{TCA Insoluble Fraction}}{\text{TCA Insoluble + TCA Soluble}} \times 100$.

TABLE 2A
Tracer Uptake by Pancreas and Liver in Obese Mice

	Body weight (g)	Pancreas uptake [^{14}C]Tryptophan % Injected dose/g	Relative conc.†‡	% TCA pellet
Control (7)	25.5 ± 1.9	44.8 ± 4.3	11.4 ± 1.1	98.9 ± 0.2
Obese (7)	39.3 ± 4.0	22.6 ± 2.5*	8.9 ± 0.9*	96.5 ± 0.6*
		^{131}I-HIPDM		
Control (6)	18.4 ± 0.8	34.5 ± 1.7	6.4 ± 0.3	
Obese (5)	36.8 ± 2.2	17.9 ± 4.4*	6.6 ± 1.6 (N.S.)	

	Liver uptake [^{14}C]Tryptophan % Injected dose/g	Relative conc.	% TCA pellet
Control (6)	4.5 ± 1.2	1.1 ± 0.3	88.0 ± 2.5
Obese (7)	1.9 ± 0.4*	0.7 ± 0.2†‡	81.8 ± 1.3*
	^{131}I-HIPDM		
Control (6)	10.2 ± 3.8	1.9 ± 0.7	
Obese (5)	5.6 ± 0.1*	2.1 ± 0.1 N.S.	

N.S. = not significant.
* $p < 0.001$.
† $p < 0.01$.
‡ relative concentration = $\frac{\text{counts/g tissue}}{\text{Injected activity/g body weight}}$.

In this study we compared the pancreas uptake of [^{14}C]TRY and [^{131}I]HIPDM in normal mice as well as various pathophysiologic models. The exocrine pancreas is one of the most active protein synthesizing organs. Therefore, most approaches to pancreatic imaging use labeled amino acids or amino acid analogs. Among them, L-tryptophan was reported to be one of the best pancreas seeking agents (*3–5*). The mechanisms for the pancreas uptake of [^{14}C]TRY has been reported to be due in part to active amino acid transport to

TABLE 2B
Tracer Uptake by Pancreas and Liver in Diabetic Mice

	Body weight (g)	Pancreas uptake [^{14}C]Tryptophan % Injected dose/g	Relative conc.**	% TCA pellet
Control (6)	21.4 ± 1.1	31.4 ± 4.5	6.8 ± 1.0	97.8 ± 0.2
Diabetic (6)	45.1 ± 2.5‡	26.9 ± 1.4 (N.S.)	12.1 ± 0.6†	97.9 ± 0.4 (N.S.)
		[^{131}I]HIPDM		
Control (6)	21.4 ± 1.1	31.5 ± 5.3	6.7 ± 1.1	
Diabetic (6)	45.1 ± 2.5‡	27.9 ± 4.6 (N.S.)	12.6 ± 1.9‡	

	Liver uptake [^{14}C]Tryptophan % Injected Dose/g	Relative Conc.	% TCA Pellet
Control (6)	3.7 ± 0.4	0.8 ± 0.1	90.5 ± 2.3
Diabetic (6)	2.4 ± 0.2†	1.1 ± 0.1‡	85.3 ± 2.2*
	[^{131}I]HIPDM		
Control (6)	7.0 ± 1.0	1.5 ± 0.2	
Diabetic (6)	4.7 ± 0.7*	2.1 ± 0.3†	

N.S. = not significant.
* $p < 0.05$.
† $p < 0.01$.
‡ $p < 0.001$.

TABLE 3
Comparison of Tracer Uptake by Tumor and Tissue at 60 min

	[^{131}I]HIPDM		[^{14}C]TRY	
	(n = 6–8) ratio		(n = 10) ratio	
	% Dose/g	Tumor/tissue	% Dose/g	Tumor/tissue
Tumor	2.29 ± 0.43	1	2.02 ± 0.67 (N.S.)	1
Liver	6.30 ± 0.58	0.36	2.58 ± 0.38	0.78
Pancreas	17.13 ± 2.17	0.13	30.03 ± 4.17	0.067
Muscle	1.52 ± 0.35	1.50	0.59 ± 0.089	3.42
Blood	1.33 ± 0.091	1.72	0.80 ± 0.10	2.53

N.S. = not significant compared to HIPDM.

pancreas cells as well as the protein synthesis for the production of digestive enzymes (*13*). In this study, we also observed that more than 95% of the injected [^{14}C] TRY was incorporated into crude protein fraction at 1 hr postinjection. Tryptophan is not included in the amino acid sequence of insulin or its precursor protein (*14*), and was reported not to accumulate in the pancreas islets (*15,16*). Thus, the pancreas uptake of L-tryptophan seems to represent the physiologic exocrine function of pancreas.

Although L-tryptophan is a metabolic precursor of serotonin and melatonin, the proportion of a dietary tryptophan converted to brain serotonin is very small (*17*). In our experiment, animals were in normal nutritional condition and study was done at 1 hr. Therefore, the fraction of the [^{14}C]TRY converted to brain serotonin is small compared to the fraction incorporated to protein, 85–99% at 1 hr.

In the alcoholic mice, chronic ethanol (20%) ingestion increased [^{14}C]TRY uptake by the pancreas after 5-wk treatment period, then decreased by 10 wk, but HIPDM distribution showed no significant differences. These findings could be due to the fact that in alcoholism there is an early stimulation followed by a suppression of the exocrine pancreas. An increased concentration of total protein in the pure pancreatic juice after chronic alcohol ingestion has been reported by several groups (*18,19*). It may lead to precipitation in pancreatic ducts and formation of protein plugs which could calcify and cause obstruction. This has been the mechanism considered the most acceptable to explain alcohol-induced chronic calcifying pancreatitis (*18*). In our study, we did not observe calcification or histological evidence of chronic pancreatitis. However, 10 wk treatment might not be enough to induce chronic calcifying pancreatitis. The increased pancreas uptake of ^{14}C-L-TRY observed after 5 wk treatment was considered to represent the functional changes of early increased protein secretion, and decreased uptake after 10 wk was consistent with the late depletion (*19*). These functional changes are expected to be induced earlier than the pathologic changes after chronic alcohol ingestion.

The obese mice are characterized by marked obesity, hypertrophy of beta-cells, hyperinsulinemia, marked insulin resistance and increased lipogenesis (*8*). The diabetic mice present with islet cell atrophy, obesity, and severe hyperglycemia (*9*). The stimulation of protein synthesis in muscle and liver is one principal actions of insulin, but in the diabetic mice accelerated protein catabolism and increased amino acid utilization for the energy production and for gluconeogenesis are parts of major metabolic changes (*14*). Increased relative concentration of [^{14}C]TRY in the diabetic pancreas can be explained either by the same mechanism or by stimulation from hyperphagia. But obese mice also have the same characteristics, and [^{14}C]TRY uptake by pancreas was decreased. In obese mice, amino acid utilization in liver might be depressed under hyperinsulinemia. The effect of endocrine abnormality on the exocrine amino acid metabolism was not straightforward, and our results showed weak correlations but further studies are needed to elucidate the point.

Neither [^{14}C]TRY nor HIPDM showed specific affinities for tumor. Tumor uptake of both isotopes was lower than the pancreas. Although we could not use tumor derived from pancreas, our results with [^{14}C] TRY were similar to the studies reported with hamsters pancreatic adenocarcinoma (*7*), and we thought there might be no significant difference between these tumors especially for comparative studies. Although some amino acids and derivatives have been used as tumor imaging agent in brain tumors (*20*) and lung cancer (*21*), L-TRY and HIPDM may not be suitable as a hot spot pancreas tumor agent, and we anticipate that tumor imaging with these tracers will produce photon deficient areas compared to the normal organ.

In a study comparing the whole-body distribution of amino acid 5-hydroxytryptophan (5HTP) and amine 5-hydroxytryptophan (5HT) it was shown that 5HTP initially accumulated in the exocrine pancreas and in organs characterized by rapid protein synthesis, viz. gastrointestinal mucosa and salivary glands. However, this pattern gradually changes and an "amine pattern" of redistribution of the amino acid occurs (*22,23*) which is characterized by localization in the adrenal medulla,

lungs, red pulp of spleen and to a certain extent, the island of Langerhans. This was thought to be due to decarboxylation of 5-HTP to 5HT.

In mammals the highest polyamine concentrations are found in regions of highest ribonucleic acid and protein synthesis, for example in prostate and pancreas (*24*). High uptake of physiological precursor [^{14}C]putrescine into pancreas has been demonstrated in vivo (*25*). Both exocrine and islet beta-cell in pancreas are responsible for these amine accumulations (*23*). Costorage of monoamine and insulin was reported but its correlation to insulin release was not clear (*26*). HIPDM is a diamine derivative, therefore its pancreas accumulation might be explained by the same transport mechanism. A small fraction might be in the islet cells of pancreas, but gross accumulation in the organ might depend on the exocrine gland, because of its relative volume in the organ. Excretion of radioactivity in the intestine at one hour after injection observed in the ARG (Fig. 2), which was almost the same as [^{14}C]TRY, support this assumption. Our results suggest that the mechanism of HIPDM uptake was not specifically correlated to pancreas physiology.

HIPDM was originally developed for a brain perfusion agent based on the pH-shift theory that at high pH this compound is neutral and lipid soluble and can diffuse freely into cells, but at the lower pH within the tissue, they become charged and can no longer diffuse out (*27*). However, the pancreas and lung uptake of HIPDM cannot be explained by the pH-shift theory because the intracellular pH of the pancreas is not low.

Our data suggest that HIPDM may be a potentially useful imaging agent for certain pancreatic diseases especially when labeled with ^{123}I which is highly suitable for conventional scintigraphy. We have not yet evaluated the species differences of HIPDM distribution in pancreas, however, few limited reports described the possible usefulness of HIPDM as a pancreas imaging agent in humans (*28*). Therefore, we believe that more detailed clinical evaluation of [^{123}I]HIPDM is warranted to determine the potential of this agent as a pancreas imaging agent in humans.

Single photon emission tomography may be required for clinical pancreas imaging with [^{123}I]HIPDM because of organ location in the body and the high liver activity which sometimes obscures part of the pancreas. Tryptophan imaging can be done only with the ^{11}C labeling using positron emission tomography. It also requires an on-site cyclotron and extensive support for radiopharmaceutical production. However, our data showed that pancreas uptake of TRY was in general higher than that of HIPDM and pancreas to liver ratios were 11.6 and 2.7 for TRY and HIPDM, respectively. The P/L ratio with ^{11}C-DL-TRY in humans is reported to be between 4 and 6 (*29*). The present data also suggest that TRY is a more sensitive indicator of various pancreatic disorders, therefore, it appears that L-tryptophan may have higher potential as a pancreas imaging agent than HIPDM.

ACKNOWLEDGMENT

The authors thank Mrs. E. L. Roche for secretarial assistance.

The submitted manuscript has been authored under contract No. DE-ACO2-76CH00016 with the United States Department of Energy. By acceptance of this article, the publisher and/or recipient acknowledges the U.S. Government's right to retain a nonexclusive, royalty-free license in and to any copyright covering this paper.

REFERENCES

1. Miale A Jr, Rodriguez-Antunez A, Gill WM Jr. Pancreas scanning after ten years. *Semin Nucl Med* 1972; 2:201–219.
2. Partain CL, Staab EV, McCartney WH. Multiple imaging modalities for the study of pancreatic disease. *Semin Nucl Med* 1979; 9:36–42.
3. Busch H, Davis JR, Honig GR, et al. The uptake of a variety of amino acids into nuclear proteins of tumors and other tissues. *Cancer Res* 1959; 19:1030–1039.
4. Buonocore E, Hübner KF. Positron-emission computed tomography of the pancreas: a preliminary study. *Radiology* 1979; 133:195–201.
5. Kirchner PT, Ryan J, Zalutsky M, et al. Positron emission tomography for evaluation of pancreatic disease. *Semin Nucl Med* 1980; 10:374–391.
6. Yamamoto K, Som P, Srivastava SC, et al. Pancreas accumulation of radioiodinated HIPDM in mice and rat. *J Nucl Med* 1985; 26:765–769.
7. Washburn LC, Sun TT, Byrd BL, et al. DL-[Carboxyl-^{11}C] tryptophan, a potential agent for pancreatic imaging; production and preclinical investigations. *J Nucl Med* 1979; 20:857–864.
8. Herbert L, Coleman DL. Laboratory animals exhibiting obesity and diabetes syndromes. *Metabolism* 1977; 26:59–99.
9. Coleman DL. Obese and diabetes: two mutant genes causing diabetes-obesity syndromes in mice. *Diabetologia* 1978; 14:141–148.
10. Yonekura Y, Brill AB, Som P, et al. Quantitative autoradiography with radiopharmaceuticals. Part 1: digital film analysis system by videodensitometry. *J Nucl Med* 1983; 24:231–237.
11. Som P, Yonekura Y, Oster ZH, et al. Quantitative autoradiography with radiopharmaceuticals. Part 2: applications in radiopharmaceutical research. *J Nucl Med* 1983; 24:238–244.
12. Woodard HQ, Bigler RE, Freed B, et al. Expression of tissue isotope distribution. *J Nucl Med* 1975; 16:958–959.
13. Bieger W, Peter S, Kern HF. Amino acid transport in the rat exocrine pancreas I. Transport of amino acids and their utilization in protein synthesis. *Cell Tissue Res* 1977; 180:31–44.
14. Martin DW, Mayes PA, Rodwell VW. Harper's review of biochemistry 18th edition. 1981: 475–483.
15. Gylfe E, Hellman B, Sehlin J, et al. Amino acid conversion into 5-hydroxytryptamine in pancreatic β-

cells. *Endocrinology* 1973; 93:932–937.
16. Howell SL, Hellerström C, Whitfield M. Radioautographic localization of labelled proteins after incubation of guinea-pig islets of Langerhans with [^{3}H] tryptophan. *Biochem J* 1974; 140:22–23.
17. Neff NH, Spano PF, Groppetti A, et al. A simple procedure for calculating the synthesis rate of norepinephrine, dopamine and serotonin in rat brain. *J Pharmacol Exp Ther* 1971; 176:701–710.
18. Sarles H, Devaux MA, Jorand MCN. Action of ethanol on the pancreas. In: Gyr KE, Singer MV, Sarles H, eds. *Pancreatitis-concepts and classification.* New York: Elsevier, 1984: 183–187.
19. Sardesai VM, Orten JM. Effect of prolonged alcohol consumption in rats on pancreatic protein synthesis. *J Nutr* 1968; 96:241–246.
20. Hübner KF, Purvis JT, Mayaley SM Jr, et al. Brain tumor imaging by positron emission computed tomography using ^{11}C-labeled amino acids. *J Comp Assis Tomogr* 1982; 6:544–550.
21. Kubota K, Matsuzawa T, Ito M, et al. Lung tumor imaging by positron emission tomography using C-11-L-methionine. *J Nucl Med* 1985; 26:37–42.
22. Tjälva H, Wilander E. The uptake in the pancreatic islets of nicotinamide nicotinic acid and typtophan and their ability to prevent streptozotocin diabetes in mice. *Acta Endocr* 1976; 83:357–364.
23. Ritzén M, Hammarstrom L, Ullberg S. Autoradiographic distribution of 5-hydroxytryptamine and 5-hydroxytryptophan in the mouse. *Biochem Pharmacol* 1965; 14:313–321.
24. Tabor H, Tabor CW. Spermidine, spermine and related amines. *Pharmacol Rev* 1964; 16:245–300.
25. Clark RB, Fair WR. The selective in-vivo incorportion and metabolism of radioactive putrescine in the adult male rat. *J Nucl Med* 1975; 16:337–342.
26. Hellman B, Lernmark A, Sehlin J, et al. Transport and storage of 5-hydroxytryptamine in pancreatic β-cells. *Biochem Pharmacol* 1972; 21:695–706.
27. Kung HF, Tramposch KM, Blau M. A new brain perfusion imaging agent: [I-123]HIPDM:N.N.N′-Trimethyl-N′-[2-hydroxy-3-methyl-5-iodobenzyl]-1,3-propanediamine. *J Nucl Med* 1983; 24:66–72.
28. Yamamoto K, Saji H, Shibata T, et al. Clinical evaluation of pancreas scintigraphy with ^{123}I-labelled HIPDM [Abstract]. *J Nucl Med* 1988; 29:826.
29. Hübner KF, Andrews GA, Buonocore E, et al. Carbon-11-labeled amino acids for the rectilinear and positron tomographic imaging of the human pancreas. *J Nucl Med* 1979; 20:507–513.